The Proapoptotic Protein tBid Forms Both Superficially Bound and Membrane-Inserted Oligomers

Sanjeevan Shivakumar,[†] Martin Kurylowicz,[‡] Nehad Hirmiz,[‡] Yaseen Manan,[†] Ouided Friaa,[‡] Aisha Shamas-Din,[†] Pourya Masoudian,[†] Brian Leber ,[†§] David W. Andrews,[†] and Cécile Fradin[†‡]*

[†]Department of Biochemistry and Biomedical Sciences, [‡]Department of Physics and Astronomy, and [§]Department of Medicine, McMaster University, Hamilton, Ontario, Canada.

SUPPORTING MATERIAL:

1. EXPERIMENTS:

1.1 Protein purification and labelling

The plasmid used in this study encoded a version of the Bid protein in which the endogenous cysteine at position 30 is replaced with a serine. This leaves only one endogenous cysteine, placed at position 126 in what becomes the tBid fragment after cleavage. The single-cysteine Bid (termed Bid 126C) was labeled as needed with thiol-reactive fluorescent dyes. The labelling efficiency was calculated by dividing the dye concentration, measured by absorption, by the protein concentration, measured either by absorption or by Bradford assay. Purified proteins were stored in storage buffer (10 mM HEPES, pH 7.2, 200 mM NaCl, 0.2 mM EDTA, 10% glycerol) at -80 ^{o}C.

1.2 Preparation of reconstituted lipid membranes

Lipid film and liposome preparation. Lipids dissolved in chloroform were combined in the right proportion and placed in a borosilicate glass tube. The chloroform was evaporated using a stream of nitrogen gas followed by vacuum drying for 2 hr. Lipid films were stored under argon at -20 ^{o}C and used within 2 weeks. To form liposomes the lipid films were hydrated to 1 mg/ml in assay buffer (10 mM HEPES pH 7, 200 mM KCl, 1 mM $MgCl_2$, and 0.2 mM EDTA). The liposome solution was then submitted to 10 freeze-thaw cycles and extruded through a polycarbonate membrane with 100 nm pores (Whatman, now GE Healthcare). Liposomes were stored at 4 ^{o}C for a maximum of 24 hours.

Mica Substrate preparation. Mica sheets with thickness between 6 and 12μm (as inferred from their mass) were cleaved from 25 mm-diameter V-1 grade mica discs (SPI Supplies, West Chester, PA) and glued to 40 mm diameter 170 μm thick glass coverslips (Bioptechs, Butler, PA) with NOA88 optical adhesive (Norland Products, Cranbury, NJ). Cleaved mica was firmly pressed on the adhesive-coated coverslip pre-heated at 50 ^{o}C in order to bring the total thickness of the coverslip, adhesive and mica assembly under 220 μm. The adhesive was then cured for 30 s under a UV lamp. Immediately prior to use the top atomic layers of the mica surface were lifted off with clear packing tape to expose a clean surface.

1.3 Steady-state fluorescence spectroscopy

To prevent protein adhesion, cuvettes were first pre-incubated for 4 hours at 37 ^{o}C with a solution of 2 mg/ml DOPC dissolved in assay buffer by overnight sonication, resulting in a surfactant-coated cuvette. After mixing the proteins (20 nM tBid-DAC and 100 nM tBid-NBD) and liposomes, the NBD fluorescence (λ_{ex} = 475 nm, λ_{em} = 530 nm), $F_{NBD}(t)$, and the DAC fluorescence (λ_{ex} = 380 nm, λ_{em} = 460 nm), $F_{DAC}(t)$, were monitored using a Quantamaster fluorometer (Photon Technology International, Birmingham, NJ). The fluorescence of NBD is

environment sensitive, such that the quantity $[F_{NBD}(t)-F_{B,NBD}]/[F_{NBD}(0)-F_{B,NBD}]$ can be used as a relative measure of hydrophobicity. In this expression $F_{B,NBD}$ is the background fluorescence measured just before the proteins have been added and $F_{NBD}(0)$ is the NBD fluorescence measured immediately after. The fluorescence of DAC, on the other hand, is related to the FRET efficiency between DAC (donor) and NBD (acceptor) through: $E = 1-[(F_{DAC+}(t)-F_{B,DAC})/(F_{DAC+}(0)-F_{B,DAC})]/[(F_{DAC-}(t)-F_{B,DAC})/(F_{DAC-}(0)-F_{B,DAC})]$, where $F_{DAC+}(t)$ is the donor fluorescence in reactions containing the acceptor cBid-NBD and $F_{DAC-}(t)$ is the donor fluorescence in reactions containing unlabelled cBid. The denominator in this expression corrects for change in fluorescence due to binding of protein to the walls of the cuvette or environment sensitivity rather than FRET, although DAC is not known to be an environment sensitive dye.

1.4 Confocal microscopy

Detection volume. The effective detection volume was assumed to be Gaussian, which means that the average fluorescence intensity detected for a particle placed at position (x,y,z) with respect to the center of the detection volume is given by:

$$\langle i(x,y,z)\rangle = Be^{-2x^2/w_0^2}e^{-2y^2/w_0^2}e^{-2z^2/z_0^2} \quad . \tag{S1}$$

In the above equation B is the specific brightness of the particle, i.e. the number of fluorescence photon per second detected on average when the particle is at the center of the detection volume. The dimensions of the detection volume were measured by performing calibration fluorescence correlation spectroscopy experiments with either Alexa 488 (diffusion coefficient D = 435 μm^2/s (1)) or Alexa 647 (D = 330 μm^2/s (2)). For imaging and fluorescence fluctuation experiments involving proteins alone or proteins in SLBs, the back-aperture of the 40× 1.15 NA water immersion objective (UApoN, Olympus) was overfilled and a 40 μm-diameter confocal pinhole was used, resulting in w_0 = 340 nm and z_0 = 2.9 μm when using a 488 nm excitation, and w_0 = 380 nm and z_0 = 2.5 μm when using a 637 nm excitation. For fluorescence fluctuation experiments involving proteins interacting with liposomes, the objective back-aperture was underfilled and a 70 μm-diameter confocal pinhole was used, resulting in a larger detection volume, more appropriate for the study of 100-nm diameter species.

Analysis of fluorescence fluctuation measurements. Measurements of solution species were performed at least 5 μm away from the mica or glass surfaces. Measurements of membrane species were performed by first acquiring an image perpendicular to the focal plane, in which the membrane could be identified as a bright line. The focal volume was then placed on the membrane and measurements were performed. In all cases, we limited the analysis to a single fluorescent species and used the general form of the autocorrelation function:

$$G(t) = \frac{1}{N}\frac{1}{\left(1+4Dt/w_0^2\right)\left(1+4Dt/z_0^2\right)^{\frac{1}{2}}}\left(1+\frac{T_1}{1-T_1}e^{-\frac{t}{\tau_{T_1}}}\right)\left(1+\frac{T_2}{1-T_2}e^{-\frac{t}{\tau_{T_2}}}\right). \tag{S2}$$

In the above formula N is the number of fluorescence particles in the effective detection volume, and T and τ_T refers to triplet state fractions and relaxation times. For membrane species the value of z_0 was set to infinity. For fluorophores for which only one dark state was present the value of T_2 was set to 0.

Membrane binding quantification. Confocal images of DiO-labelled SLBs incubated for 15 min at 37 °C with different concentrations of cBid-Atto647 (between 1 and 30 nM) were acquired perpendicular to the plane of the membrane. By taking into account the fluorescence background intensity measured in the absence of protein, the average intensity in the membrane, $\langle I_M \rangle$, and the average intensity in solution, $\langle I_S \rangle$, were extracted from the average fluorescence intensity profiles along the optical axis. Assuming a 3D Gaussian volume (Eq. S1), these quantities are related to the concentration of tBid inside the membrane (in molecule/m^3), $[tBid_M]_M$, and its concentration in solution (also in molecule/m^3), $[tBid]_S$, through the expressions: $\langle I_S \rangle = [tBid]_S B(\pi/2)^{3/2} w_0^2 z_0$ and $\langle I_M \rangle = \langle I_S \rangle/2 + [tBid_M]_M B(\pi/2) w_0^2 d$, where d is the membrane thickness (3).

The partition of the protein between membrane and solution is characterized by the partition coefficient, $P_{M/S} = [\mathrm{tBid_M}]_M/[\mathrm{tBid}]_S$, which can be expressed as a function of the measured intensities:

$$P_{M/S} = (\pi/2)^{1/2} \frac{z_0}{d} \left(\langle I_M \rangle / \langle I_S \rangle - 1/2 \right) \tag{S3}$$

We can also describe the partition of the protein between solution and membrane as a simple binding equilibrium (see section 3.1 for a detailed discussion of the equivalence between these two description). The associated dissociation constant is $K_D = [tBid]_S [L]/[tBid_M]$, where [L] is the lipid concentration (again, in molecule/m^3) and where the concentration of membrane-associated tBid is $[tBid_M] = [tBid_M]_M [L] dA/2$. The constant A = 0.75 nm^2 is the average surface area of a single lipid. This leads to:

$$K_D = \frac{2[tBid]_S}{Ad[tBid_M]_M} = \frac{2^{3/2}}{\left(\langle I_M \rangle / \langle I_S \rangle - 1/2 \right) \pi^{1/2} A z_0} = \frac{C}{\left(\langle I_M \rangle / \langle I_S \rangle - 1/2 \right)} , \tag{S3'}$$

where $C = 2^{3/2} / \left(\pi^{1/2} A z_0 \right)$. For a value of the aspect ratio z_0 = 2.5 ± 0.5 µm we get $C = (8.5 \pm 1.5) \times 10^{23}$ molecule/m^3 or $C = (1400 \pm 300) \mu M$.

1.5 Atomic force microscopy

Fully hydrated single supported lipid bilayers were imaged with a Bruker BioScope Catalyst BioAFM system used in PeakForce Tapping Mode. The membranes were prepared directly inside the instrument fluid sample cell, which was equipped with a temperature controlled stage, by incubating a 1 mg/ml liposome solution for 20min at 37 °C on freshly cleaved mica. Image acquisition was then also performed at 37 °C. The PeakForce module works by generating images from force-distance curves acquired at each pixel. This allows for ultralow force imaging (<50 pN) on soft samples, without the need to tune cantilever resonance or drive amplitude. The ScanAsyst module of the instrument was used to automatically set operational parameters, including integral gain, proportional gain and amplitude setpoint. The typical scan rate used was 1.5 Hz for a scan size of 10×10 µm. An image of a mitochondria-like supported membrane is presented in supplementary Fig. S1.

2. SINGLE PARTICLE DETECTION:

2.1 Single particle detection of mobile and immobile objects in confocal images

The brightest image in the stack was first selected as most likely to be acquired exactly in the plane of the membrane. Two copies of the image were kept, one for event detection (detection image) and one for event characterization (fitting image). The pixel with highest intensity in the detection image (excluding a 7 pixel band along the borders of the image) was selected and a *10x10*-pixel region of interest (ROI) defined around that pixel in the fitting image. This ROI was then subjected to a 6-parameter 2D-Gaussian fit according to the equation:

$$I_{fit}(x,y) = i_B + i_{\max} e^{-2(x-x_0)^2/w_x^2} e^{-2(y-y_0)^2/w_y^2} \quad \text{(S4)}$$

The amplitude i_{max}, noise level i_B, widths w_x and w_y, and peak positions x_0 and y_0 of this particular event were obtained by minimizing the normalized chi-squared:

$$\chi_N^2 = \frac{1}{n^2-6} \sum_{j=1}^{n} \sum_{k=1}^{n} \frac{\left(i(j,k) - I_{fit}(x_j, y_k)\right)^2}{I_{fit}(x_j, y_k)} \quad \text{(S5)}$$

where n is the dimension of the ROI, $i(j,k)$ is the number of photons detected in the pixel with index j and k within that ROI, and x_j and y_k are the coordinates of the center of that pixel. The precision achieved for i_{max} was better than 30% for events with S/N of 3 or more. The fit was then repeated a second time with a new ROI centered at the position (x_0, y_0) returned by the first fit. Once the final values of the Gaussian parameters were obtained, a *4x4* square of pixels was removed from the detection image before identifying the pixel with the next highest intensity. If this pixel had the largest value within the ROI around it as extracted from the fitting image (now different from the detection image since no pixel have been removed), then the fitting procedure was executed as above. If there was a pixel with higher intensity in the ROI, then a *4x4* square of pixels was removed around this maximum in the detection image with no fitting and the next maximum was found. After each fit the value for the noise, *z,* was added to a running average $\langle i_B \rangle$ to determine the noise floor of the image. A threshold intensity value was computed $p = \langle i_B \rangle + B/2$ to determine when to stop collecting local maxima, where B is the specific brightness of a protein monomer as measured in solution by FIDA.

Events were classified according to the values and aspect ratio of w_x and w_y. Spots were identified as events for which:

$$\left[\left(w_x - w_0\right)^2 + \left(w_y - w_0\right)^2 \right]^{1/2} \le w_0/2 \,. \quad \text{(S6)}$$

Horizontal streaks were identified as events for which $w_y < w_0/2$. Events not identified as diffraction-limited spots or horizontal streaks, which may have corresponded to multiple particles too close to be resolved, particles near the border of the image or out-of-focus particles, were rejected.

2.2 Obtaining distribution of oligomer stoichiometry from events intensity

Normalized intensity distribution, $P^A(n)$. For each event, the apparent specific brightness captured, i_{max}, was normalized by the specific molecular brightness of a monomer, B. This normalization resulted into a continuous distribution of normalized apparent specific brightness, $P^A(n)$, where normalized intensity $n = i_{\max}/B$ could take non-integer values.

Normalized specific brightness distribution, $P^A(N)$. In the case of immobile particles the apparent specific brightness may differ from the actual specific brightness (expected to be a multiple of B) because of photon noise. Thus particles composed of n fluorophores have normalized apparent specific brightness with values distributed around n. We assumed this distribution was close to normal, and we therefore fitted the normalized intensity distribution obtained for immobile particles with a sum of Gaussian functions:

$$P_{Immobile}(n) = \frac{1}{\sqrt{2\pi\sigma}} \sum_{N=1}^{6} a_N e^{-\frac{\left[n-\left(n_1+(N-1)\Delta n\right)\right]^2}{2\sigma^2}} \tag{S7}$$

which returned the normalized apparent specific brightness of the dimmest particles, n_1, the increment in normalized apparent specific brightness between particles of different brightness, Δn, the width of the distributions, σ, and the number of events associated with the actual normalized specific brightness N, a_N. This allowed constructing a discrete distribution of normalized specific brightness, $P^A(N) = a_N$, where N only takes integer values.

In the case of mobile particles, captured only for one line in confocal images and appearing as horizontal streaks, a normal distribution of apparent normalized specific brightness around the expected integer value is not appropriate since the particle is most likely to have crossed the detection volume away from its center. Following a similar line of reasoning as in (4), we find that the apparent specific brightness distribution for particles with motion restricted in the focal plane should be:

$$p\left(B, i_{\max}\right) = \frac{1}{2\left[\ln\left(B/t_D\right)\right]^{1/2}\left[\ln\left(B/i_{\max}\right)\right]^{1/2} i_{\max}} \ , \tag{S8}$$

where the apparent specific brightness, i_{max}, can take any value between the detection threshold value, t_D, and the actual specific brightness, B. Again taking into account photon noise by considering a normal distribution around the expected specific brightness values, and again considering a particle population with specific brightness that are multiple of B, we obtained a function for the distribution of apparent normalized specific brightness for mobile particles:

$$P_{Mobile}(n) = \frac{1}{\sqrt{2\pi\sigma}} \sum_{N=1}^{6} b_N \int_{t_D}^{\left[n_1+(N-1)\Delta n\right]B} p\left(\left[n_1+\left(N-1\right)\Delta n\right]B, x\right) e^{-(nB-x)^2/\left(2\sigma^2\right)} dx \tag{S9}$$

A fit of the data to Eq. 9 returned the number of events associated with the actual normalized specific brightness N, b_N, and allowed constructing a discrete distribution of normalized specific brightness, $P^A(N) = b_N$, for mobile particles.

Oligomer stoichiometry distribution, $P^T(N)$. The discrete normalized specific brightness distribution, $P^A(N)$, may be different from the true stoichiometry distribution, $P^T(N)$, because

some proteins in a protein assembly may not have a functioning fluorophore, both because of incomplete labeling efficiency and because of photobleaching. If the fraction of labeled proteins, f, is known it is however possible to calculate $P^T(N)$. For a given stoichiometry, N, the probability that k proteins in the assembly are unlabelled is $f^{N-k}(1-f)^k$. Using the binomial coefficients to count states we can express the apparent stoichiometry distribution as a function the true stoichiometry distribution:

$$P^A(N) = \sum_{k=N-1}^{\infty} \binom{k}{N} f^{N-k}(1-f)^k P^T(k). \tag{S10}$$

In practice, this system of linear equation was truncated at $k = 10$ and solved using Mathematica in order to retrieve the true stoichiometry distribution, $P^T(N)$. For each separate experiment, the labeling efficiency measured for the batch of proteins used in that particular experiment was used, and photobleaching effects were neglected since imaging conditions were optimized to avoid them.

Note that the correction grows in significance for larger oligomers since the size of the correction grows as a power of N, while the error on the true distribution grows as the labeling efficiency, f, decreases, outlining the importance of achieving high labeling efficiencies

Coincidental particle detection. At the subnanomolar cBid concentration used for the presented experiments, the total concentration of tBid complexes at the membrane surface was ~0.5 μm^{-2}, or ~0.2 per pixel. This means there is only a ~10% chance for each detected event to have resulted from the coincidental presence of two particles within the same pixel, and less than 1% chance to have resulted from the presence of three particles (4, 5). The coincidental detection of particles could therefore be neglected.

3. MODELING:

3.1 Membrane binding equilibrium

The distribution of a molecule between two phases is often described in term of the partition coefficient, P, that is the ratio of concentrations of the molecule in either phase. In that context, the partition of cleaved Bid between a solution species, cBid, and a membrane species, $tBid_M$, can be characterized by the coefficient:

$$P_{M/S} = [tBid_M]_M / [cBid]_S . \quad \text{(S11)}$$

In the above, $[tBid_M]_M$ is the concentration of $tBid_M$ in the membrane phase, while $[cBid]_S$ is the concentration of $cBid$ in the aqueous phase. Both concentrations are volume concentrations, with dimension m^{-3}. To first order, the partition coefficient is expected to be a constant.

The volume of the aqueous phase, V_S, is almost identical to the total volume of the sample, V_T. Thus $[cBid]_S \approx [cBid]$, where $[cBid]$ is the overall concentration of soluble cBid in the sample. On the other hand, the volume of the lipid phase, V_M, is related to the overall lipid concentration, $[L]$, and to the average surface area (A) and length (d/2) of a lipid, through: $V_M / V_T = [L]Ad/2$. Thus $[tBid_M] = [tBid_M]_M [L] Ad/2$. This means Eq. S11 can be rewritten as:

$$\frac{[cBid][L]}{[tBid_M]} = \frac{2/(Ad)}{P_{M/S}} \quad \text{(S12)}$$

Eq. S12 is equivalent to a binding equilibrium (free ligand approximation) between the soluble form of the protein (cBid) and the lipids, with an apparent dissociation coefficient $K_D = 2/(AdP_{M/S})$. Note that the constant 2/(Ad) is simply the volume of a lipid. Thus, although the protein and the lipids do not actually undergo a bimolecular reaction, the system can be formally treated as a simple equilibrium between the two species. The advantage of this formalism is that it allows explicitly calculating the fraction of bound protein as a function of lipid concentration.

Considering that A = 0.75 nm^2 and d = 4 nm, the relationship between the partition coefficient and the apparent dissociation constant is: $K_D \approx (1.1M)/P_{M/S}$.

3.2 Simple membrane dimer formation model

To improve on the partition model described in the previous section by taking into account the possibility of tBid dimer formation, a model was formulated by considering five different tBid species: Soluble tBid in complex with the p7 fragment (cBid), soluble tBid dimers ($tBid_2$), loosely membrane-associated tBid ($tBid_{MA}$), membrane-inserted tBid ($tBid_{MI}$) and membrane inserted tBid dimers ($tBid_{MI,2}$). These species interact through the following four equilibria, as illustrated in Fig. 1D:

$$2\, cBid \leftrightarrow tBid_2$$

$$cBid + lipids \leftrightarrow tBid_{MA}$$

$$tBid_{MA} \leftrightarrow tBid_{MI}$$

$$2\ tBid_{MI} \leftrightarrow tBid_{MI,2}$$

This leads to the following set of five equations, which include four equations derived from the law of mass action for the above four equilibrium reactions, and one equation for the conservation of matter applied to tBid:

$$K_{D,2} = [cBid]^2/[tBid_2] \quad \text{(S13a)}$$

$$K_{D,1} = [cBid][L]/[tBid_{MA}] \quad \text{(S13b)}$$

$$K = [tBid_{MI}]/[tBid_{MA}] \quad \text{(S13c)}$$

$$2D - K_{D,3} = 2[tBid_{MI}]^2/\left([L]A\left[tBid_{MI,2}\right]\right) \quad \text{(S13d)}$$

$$c_0 = [cBid] + 2[tBid_2] + [tBid_{MA}] + [tBid_{MI}] + 2\left[tBid_{MI,2}\right] \quad \text{(S13e)}$$

In the above equations brackets denote the overall concentrations in the sample of the concerned form of the protein, expressed in M. $[L]$ is the total lipid concentration, assumed to be constant (i.e. always in excess) and c_0 is the total tBid concentration. The surface concentration of membrane species, for example $tBid_{MA}$, can therefore be expressed as $[tBid_{MA}]_S = 2[tBid_{MA}]/([L]A)$ where A is the average surface area occupied by a lipid in the bilayer leaflet.

The above system of equation was solved, using Mathematica (Wolfram Research, Champaign, IL), to obtain the relative fractions of *cBid*, $tBid_2$, $tBid_{MA}$, $tBid_{MI}$ and $tBid_{MI,2}$., as a function of $[L]$ and c_0. The obtained analytical solutions were then used to perform a global fit of the data presented in Fig. 1E, F and G, returning the best values for the equilibrium constants $K_{D,1}$, $K_{D,2}$, K and 2D-$K_{D,3}$, as well as the maximum FRET efficiency that would be obtained if all the proteins were forming dimers.

4. SUPPLEMENTARY FIGURES:

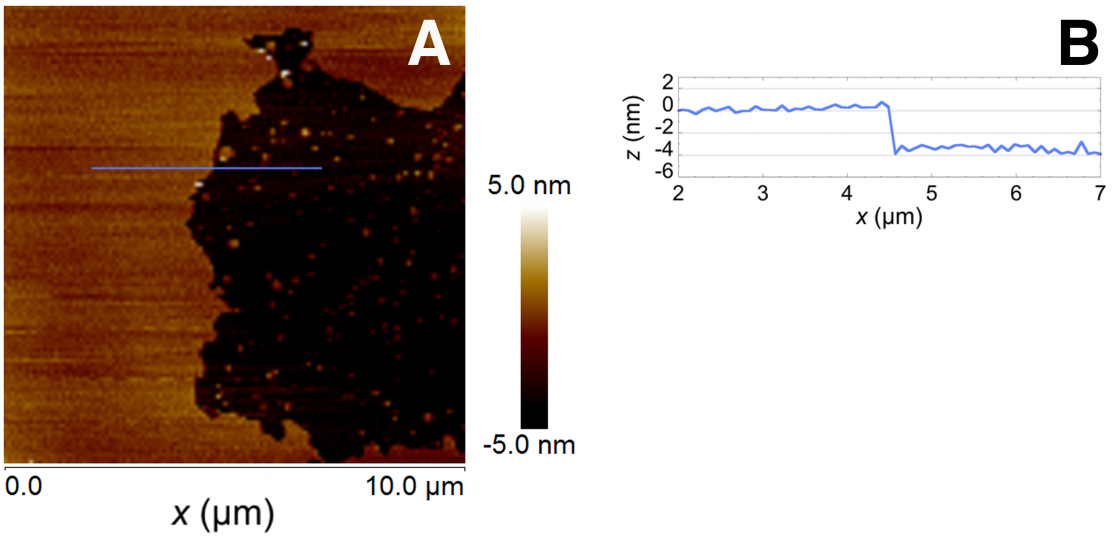

Figure S1: Atomic force microscopy image of a mitochondria-like supported lipid bilayer. (A) Height image of a 10×10 µm area of a mitochondrial-like supported lipid bilayer acquired in buffer at 37 ^{o}C. This image was selected because it shows a patch of bare mica (black area), allowing the measurements of the lipid bilayer thickness. As expected for a fluid bilayer with no large-scale lipid domains, the part of the image corresponding to the lipid membrane (orange area) does not show any visible features. (B) Height profile obtained for the cross-section of the image outlined by the blue line in (A). The value obtained for the thickness of the membrane (~ 4 nm) confirms that it is made of a single lipid bilayer.

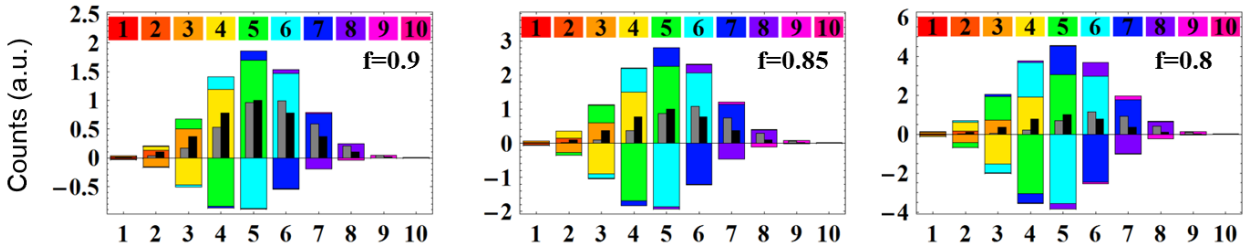

Figure S2: Decomposition of the correction for fluorophore labelling efficiency, as described by Eq. S10. Transformation of a Gaussian $P^A(N)$ (black) centred at N = 5 to the true distribution $P^T(N)$ (gray) centred at N > 5, for fluorophore labelling efficiencies f = 0.8 (left), f = 0.85 (centre) and f = 0.9 (right). The coloured bars behind each black and gray pair represent the contributions to $P^T(N)$ from $P^A(N)$, where each N in $P^A(N)$ is colour coded according to the legend at the top of the figure. The gray bars showing the true distribution, $P^T(N)$, are obtained by summing over all the coloured bars shown behind them, which represent the contributions from the apparent oligomers with stoichiometry equal to N or larger P^A. The shift of the observed peak in $P^A(N)$ to higher values of N in $P^T(N)$ grows with decreasing labelling efficiency, as do the size of the positive and negative terms in the correction, and therefore the error on the true distribution.

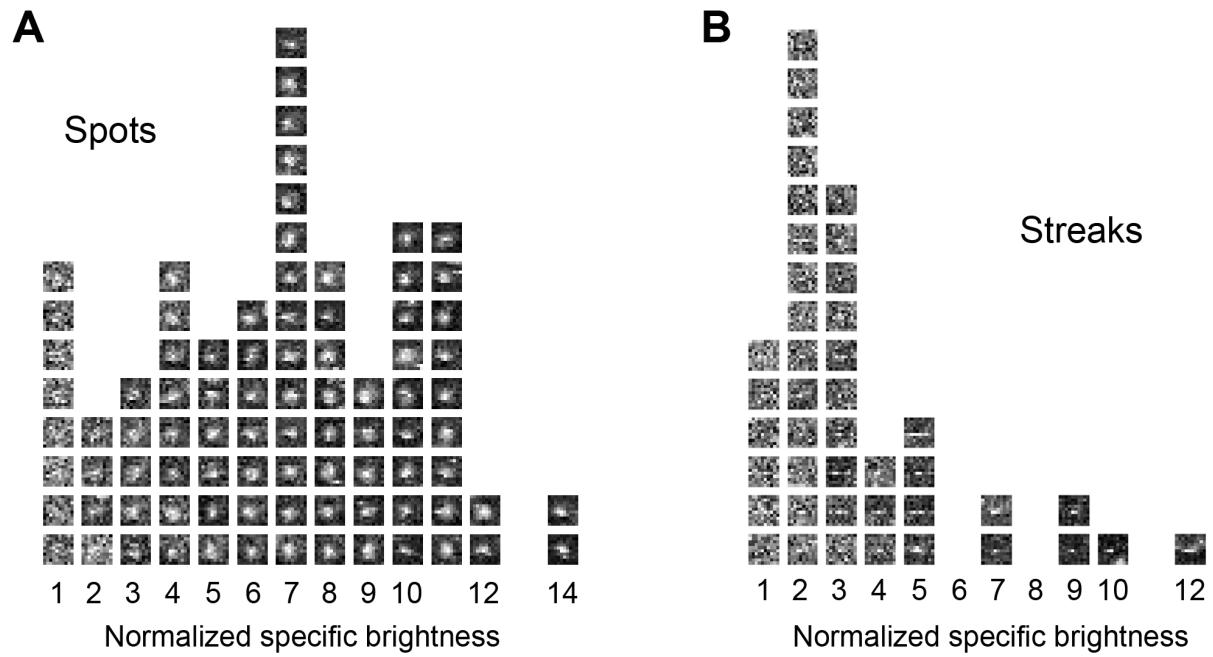

Figure S3: Examples of detected events in confocal images of tBid bound to a mitochondria-like SLB. Examples of events classified as **(A)** spots or **(B)** streaks, organized according to their apparent stoichiometry (normalized specific brightness). The number of shown events for a specific apparent stoichiometry is proportional to the total number of events detected in that sample for that stoichiometry.

5. SUPPORTING REFERENCES:

1. Petrasek, Z., and P. Schwille. 2008. *Precise measurement of diffusion coefficients using scanning fluorescence correlation spectroscopy*. Biophysical journal 94:1437-1448.
2. Loman, A., C. B. Muller, F. Koberling, W. Richtering, and J. Enderlein. 2008. *Absolute and precise measurements of the diffusion of small fluorescent dye molecules across the visible spectrum*. Poster, 14th International Workshop on Single Molecule Spectroscopy and Ultrasensitive Analysis in Life Sciences.
3. Abu-Arish, A., P. Kalab, J. Ng-Kamstra, K. Weis, and C. Fradin. 2009. *Spatial distribution and mobility of the Ran GTPase in live interphase cells*. Biophysical journal 97:2164-2178.
4. Friaa, O., M. Furukawa, A. Shamas-Din, B. Leber, D. W. Andrews, and C. Fradin. 2013. *Optimizing the Acquisition and Analysis of Confocal Images for Quantitative Single-Mobile-Particle Detection*. Chemphyschem : a European journal of chemical physics and physical chemistry 14:2476-2490.
5. Kasai, R. S., K. G. N. Suzuki, E. R. Prossnitz, I. Koyama-Honda, C. Nakada, T. K. Fujiwara, and A. Kusumi. 2011. *Full characterization of GPCR monomer-dimer dynamic equilibrium by single molecule imaging.* J. Cell Biol. 192:463-480.